

Measurements of the CKM angle γ and parameters related to mixing and CP violation in the charm at LHCb

Innes Mackay¹ on behalf of the LHCb Collaboration

¹University of Oxford, Oxford, United Kingdom

April 30, 2024

Abstract

A recent combination of measurements performed by the LHCb collaboration determined that $\gamma = (63.8^{+3.5}_{-3.7})^\circ$. The fit combined the results of γ and charm measurements, which resulted in precision improvements for the strong-phase difference between $D^0 \rightarrow K^- \pi^+$ and $D^0 \rightarrow K^+ \pi^-$ decays, $\delta_{K\pi}^D$, and the D^0 – \bar{D}^0 mixing parameter, y . In addition, new LHCb measurements of the CKM angle γ using $B^0 \rightarrow DK^{*0}$ and $B^- \rightarrow D^* K^-$ decays with the $D \rightarrow K_S^0 h^+ h^-$ final state (where $h = \pi, K$) are presented.

1 LHCb combination of γ and charm measurements

A key goal of flavour physics is to test the unitarity of the CKM matrix by overconstraining the Unitarity Triangle (UT). The angle γ is particularly interesting because it can be measured with a negligible theoretical uncertainty using tree-level decays [1]. The direct measurements of γ are compared to indirect determinations from global fits to parameters related to the other angles and sides of the UT [2, 3] that are measured in decays with additional loop diagrams. Discrepancies between the direct and indirect measurements of γ would be a sign of beyond Standard Model effects.

The angle γ is most precisely measured using $B^- \rightarrow DK^-$ decays, where D is a superposition of D^0 and \bar{D}^0 mesons. The ratio of amplitudes for the two decay paths is

$$r_B e^{i(\delta_B - \gamma)} = \frac{A(B^- \rightarrow \bar{D}^0 K^-)}{A(B^- \rightarrow D^0 K^-)}, \quad (1.1)$$

where r_B and δ_B are the amplitude ratio and strong-phase difference between the decays. The angle γ can be determined by exploiting interference between $B^- \rightarrow D^0(\rightarrow f)K^-$ and $B^- \rightarrow \bar{D}^0(\rightarrow f)K^-$ decays, where f is a common final state to both D^0 and \bar{D}^0 mesons. The same equations above apply to $B^+ \rightarrow DK^+$ decays under the exchange $\gamma \rightarrow -\gamma$. The procedure can be generalised to B^0 and B_s^0 decays, because the sensitivity to γ originates from the interference between $b \rightarrow u$ and $b \rightarrow c$ quark transitions that is shared by all B -meson decays into a mixture of D^0 and \bar{D}^0 decays.

The squared amplitude for the $B^- \rightarrow D(\rightarrow f)K^-$ decay is

$$|A(B^-)|^2 \propto A_D^2 + r_B^2 A_{\bar{D}}^2 + 2A_D A_{\bar{D}} r_B \cos(\delta_B + \delta_D - \gamma), \quad (1.2)$$

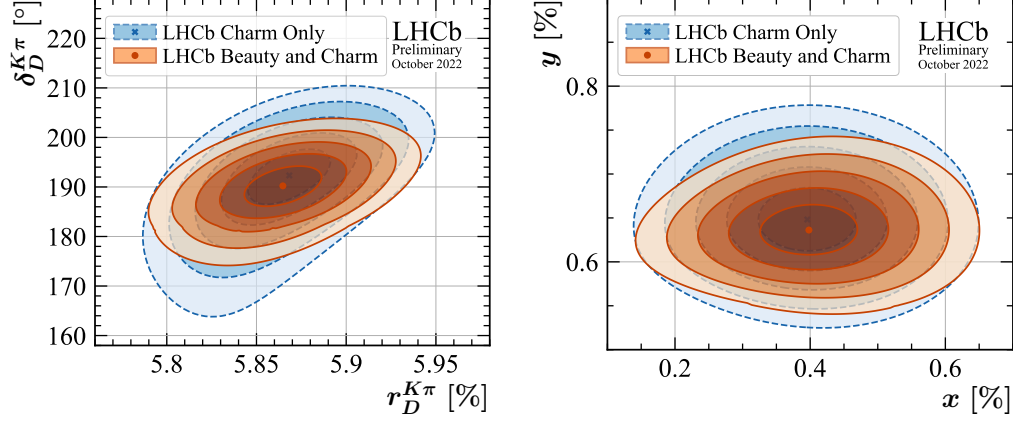


Figure 1: Comparison between the 1 (68.3%) to 5σ confidence regions for (left) $r_{K\pi}^D$ vs. $\delta_{K\pi}^D$ and (right) x vs. y , as determined in a combination of LHCb γ and charm measurements (orange) and charm only (blue) [5].

where A_D and $A_{\bar{D}}$ are the magnitude of the amplitudes for the $D^0 \rightarrow f$ and $\bar{D}^0 \rightarrow f$ decays, respectively, and δ_D is the strong-phase difference between them. Therefore, external knowledge of the D decay amplitudes is used to extract γ . The specific inputs depend on the final state of the D decay, and are most often expressed in terms of the amplitude ratio, r_D , and strong-phase difference, δ_D , between the $D^0 \rightarrow f$ and $\bar{D}^0 \rightarrow f$ decays. The reverse scenario is also possible, such that the results of the γ analyses can be used to constrain the values of δ_D and r_D . This is particularly useful for the $D^0 \rightarrow K^-\pi^+$ final state, because the determination of the D^0 – \bar{D}^0 mixing parameters, x and y , in this decay channel require knowledge of the strong-phase difference $\delta_{K\pi}^D$ [4]. In 2021, the LHCb collaboration combined the results of the γ measurements with those in the charm quark sector, which determined a noticeable improvement in the precision of $\delta_{K\pi}^D$ and y , as is displayed in Fig. 1 [5].

In the combination γ was determined to be $\gamma = (63.8^{+3.5}_{-3.7})^\circ$, which is in good agreement with the indirect measurements $\gamma = (65.6^{+0.9}_{-2.7})^\circ$ [2] or $\gamma = (65.8 \pm 2.2)^\circ$ [3] depending on the statistical approach used. A comparison of γ measurements using different B meson decays is displayed in Fig. 2. Those that use B^\pm mesons dominate the precision and are in minor tension with measurements made using B_s^0 and B^0 decays. However, recent results using time-dependent B_s^0 decays [6] and time-independent B^0 decays [7, 8], which both use the full LHCb dataset, will see better agreement in the next combination. Furthermore, additional sensitivity to γ will be achieved by including the results of two measurements made using the $B^\pm \rightarrow D^*K^\pm$ channel for the first time [9, 10]. The remainder of these proceedings will discuss some of the new LHCb measurements of γ that use the $D \rightarrow K_S^0 h^+ h^-$ decay final state, where $h = \pi, K$.

2 Measuring γ with $D \rightarrow K_S^0 h^+ h^-$ final states

The amplitude for the $D \rightarrow K_S^0 h^+ h^-$ decay is phase-space dependent due to intermediate resonances. It is found that the sensitivity to γ is optimised by studying regions of this phase space, which is categorised by the squared invariant masses of the $K_S^0 h^+$ and $K_S^0 h^-$

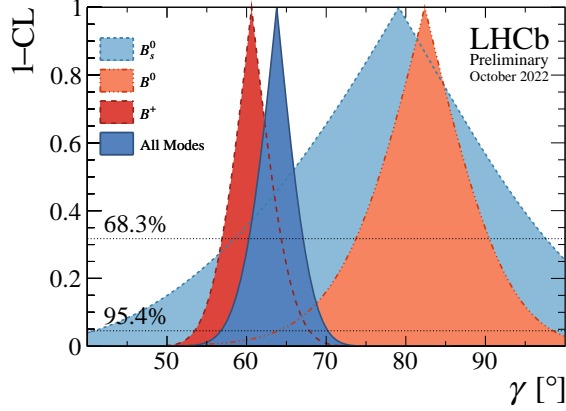


Figure 2: Confidence levels for values of the CKM angle γ determined in a combination of γ and charm measurements at LHCb. The confidence levels for γ measured using (red) B^\pm , (orange) B^0 , (light blue) B_s^0 and (dark blue) all B decays are shown [5].

pairs, labelled m_+^2 and m_-^2 , respectively [11–14]. The phase space is divided into $2\mathcal{N}$ regions labelled from $i = -\mathcal{N}$ to $i = \mathcal{N}$ (excluding 0), and is symmetrical about the line $m_-^2 = m_+^2$, where a region with $m_-^2 > m_+^2$ ($m_-^2 < m_+^2$) is the i^{th} ($-i^{th}$) bin. For the $D \rightarrow K_S^0 \pi^+ \pi^-$ ($D \rightarrow K_S^0 K^+ K^-$) decay a scheme with $\mathcal{N} = 8$ ($\mathcal{N} = 2$) regions is used [15].

The signal yields in a phase-space region, i , are given by

$$N_i(B^- \rightarrow DK^-) = h^{B^-} \left[F_i + (x_-^2 + y_-^2)F_{-i} + 2\sqrt{F_i F_{-i}}(c_i x_- + s_i y_-) \right], \quad (2.1)$$

$$N_i(B^+ \rightarrow DK^+) = h^{B^+} \left[F_{-i} + (x_+^2 + y_+^2)F_i + 2\sqrt{F_i F_{-i}}(c_i x_+ - s_i y_+) \right], \quad (2.2)$$

where x_\pm and y_\pm are the CP violation observables defined as $x_\pm = r_B \cos(\delta_B \pm \gamma)$ and $y_\pm = r_B \sin(\delta_B \pm \gamma)$. Furthermore, the h^{B^\pm} are normalisation factors which absorb the detector effects and production asymmetries, the F_i parameters are the efficiency corrected probabilities for a $D^0 \rightarrow K_S^0 h^+ h^-$ decay in a phase-space region, i , and the parameters c_i and s_i are given by integrals over the D decay amplitude averaged cosines and sines of the strong-phase difference, δ_D ,

$$K_i = \int_i dm_-^2 dm_+^2 |A_D(m_-^2, m_+^2)|^2, \quad (2.3)$$

$$c_i = \frac{1}{\sqrt{K_i K_{-i}}} \int_i dm_-^2 dm_+^2 |A_D(m_-^2, m_+^2)| |A_{\bar{D}}(m_-^2, m_+^2)| \cos \delta_D(m_-^2, m_+^2), \quad (2.4)$$

$$s_i = \frac{1}{\sqrt{K_i K_{-i}}} \int_i dm_-^2 dm_+^2 |A_D(m_-^2, m_+^2)| |A_{\bar{D}}(m_-^2, m_+^2)| \sin \delta_D(m_-^2, m_+^2). \quad (2.5)$$

The γ measurements presented in these proceedings do not rely on amplitude models for the c_i and s_i inputs. Instead, they are determined using quantum-correlated $D^0 \bar{D}^0$ pairs produced at charm factories [16, 17]. In each measurement, fits to the B and \bar{B} meson invariant mass distributions in each phase-space region are performed with the signal yields parameterised by equations Eqs. 2.1 and 2.2 to extract values for the CP violation observables and thus γ , r_B and δ_B .

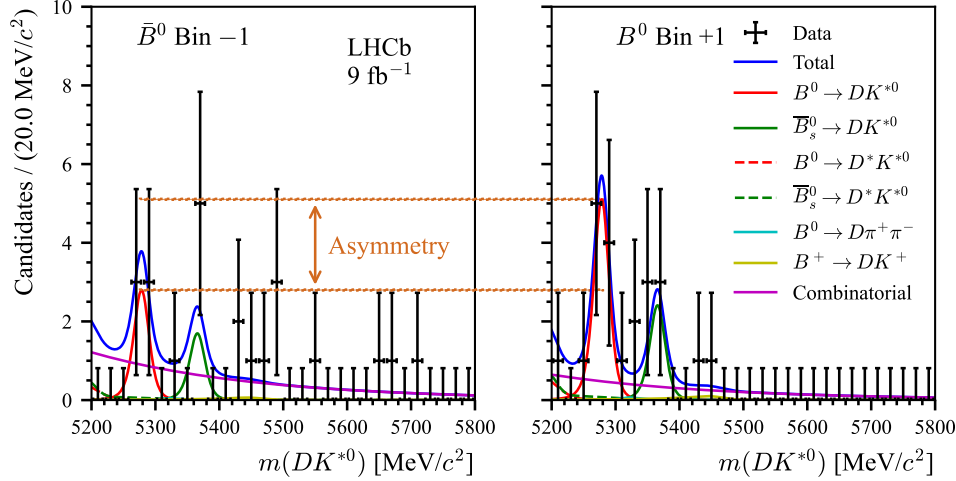


Figure 3: Fit to the distribution of $\bar{B}^0 \rightarrow D\bar{K}^{*0}$ candidates in the phase-space region, $i = -1$, compared to that of $B^0 \rightarrow DK^{*0}$ decays in the phase-space region, $i = +1$. The asymmetry is highlighted on the plot.

3 Measuring γ in $B^0 \rightarrow DK^{*0}(892)$ decays

The measurement of γ using $B^0 \rightarrow DK^{*0}(892)$ decays [7] is performed without accounting for time dependence because the flavour of the B^0 meson at decay is unambiguously tagged by the charge on the kaon from the $K^{*0} \rightarrow K^+\pi^-$ decay. Both paths to the $B^0 \rightarrow DK^{*0}$ decay final state are colour suppressed, whereas only one is in $B^- \rightarrow DK^-$ decays. Therefore, the interference in $B^0 \rightarrow DK^{*0}$ decays is expected to be around 3 times larger and thus each event has a higher sensitivity to γ compared to $B^- \rightarrow DK^-$.

Criteria are imposed to select the $B^0 \rightarrow DK^{*0}$ resonance in the $B^0 \rightarrow DK^+\pi^-$ phase space. However, non-signal decays still remain in this region which need to be accounted for. This is achieved by introducing a coherence factor, $\kappa = 0.958^{+0.005}_{-0.046}$ [18], which dilutes the interference terms in Eqs. 2.1 and 2.2. In the fit to data, the F_i values are fixed to those determined in $B^- \rightarrow D\pi^-$ decays determined in Ref. [19]. The relative efficiency differences across the phase space between $B^0 \rightarrow DK^{*0}$ and $B^- \rightarrow D\pi^-$ decays are examined in simulation and found to be small. Figure 3 compares the fit to $B^0 \rightarrow DK^{*0}$ candidates in the phase-space region $i = 1$, with that of $\bar{B}^0 \rightarrow D\bar{K}^{*0}$ candidates in the phase-space region $i = -1$, to provide an example of the CP asymmetry. The analysis determines that

$$\begin{aligned}\gamma &= (49^{+22}_{-19})^\circ, \\ r_{B^0} &= 0.271^{+0.065}_{-0.066}, \\ \delta_{B^0} &= (236^{+19}_{-21})^\circ,\end{aligned}$$

where the uncertainties are statistically dominated. The values presented supersede those determined using a smaller dataset in Ref. [20]. The measurement is required to break the four fold degeneracy of γ values from measurements of $B^0 \rightarrow DK^{*0}$ decays with D decays to 2- and 4-body final states presented in Ref. [8]. The combined precision is around 7° , with a best-fit value that will reduce the tensions with measurements performed using B^\pm decays.

Parameter	Fully reconstructed	Partially reconstructed
γ	$(69^{+14}_{-14})^\circ$	$(92^{+21}_{-17})^\circ$
r_{B^+}	0.15 ± 0.03	$0.080^{+0.022}_{-0.023}$
δ_{B^+}	$(311 \pm 15)^\circ$	$(310^{+15}_{-20})^\circ$

Table 1: Fitted values of γ and the hadronic parameters determined using fully and partially reconstructed $B^\mp \rightarrow D^*K^\pm$ decays.

4 Measuring γ using $B^\pm \rightarrow D^*K^\pm$ decays

Two new measurements of γ using $B^- \rightarrow D^*K^-$ decays have recently been performed by the LHCb collaboration. The study presented in Ref. [10] reconstructs the full decay chain, whilst that described in Ref. [9] does not reconstruct the soft neutral particle from the $D^* \rightarrow DX$ decay, where $X = \pi^0, \gamma$. There are advantages and disadvantages to both measurements. In the former, the signal yield is lower because the reconstruction efficiency of soft neutral particles is low at LHCb; however, it has fewer backgrounds and they are easier to distinguish.

In each measurement, $B^- \rightarrow D^*\pi^-$ decays are used as an additional signal channel. The interference in these decays is small, so they don't significantly contribute to the measurement of γ . Instead, they are used to determine the F_i values which are simultaneously fitted alongside the CP violation observables.

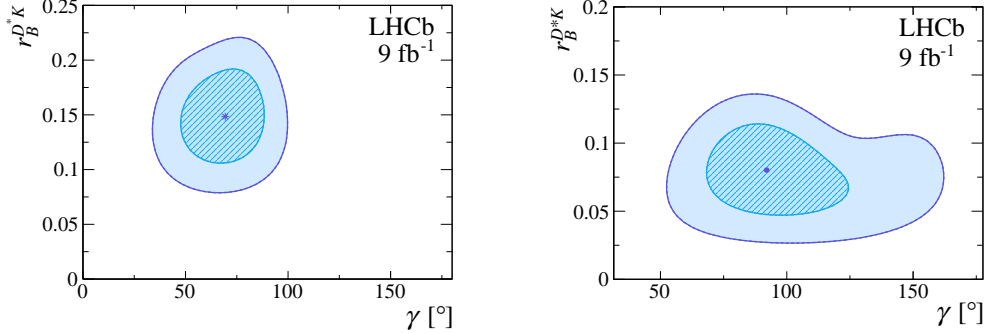


Figure 4: The 68.3% and 95.5% confidence regions in the γ vs. r_{B^0} plane determined in the fits to the CP violation observables in the study of (left) fully reconstructed and (right) partially reconstructed $B^\pm \rightarrow D^*K^\pm$ decays.

The values of γ , r_B and δ_B determined in each analysis are displayed in Tab. 1. The two measurements are found to be statistically independent. The results are in agreement with each other, and with the average value of γ determined in the LHCb combination [5]. Figure 4 displays a comparison between the 68.3% and 95.5% confidence regions in the γ vs. r_{B^+} plane in both measurements. The uncertainty on γ is inversely proportional to the value of r_{B^+} determined in the fit, which leads to larger confidence regions in the γ vs. r_{B^+} plane for the partially reconstructed analysis despite the CP violation observables being more precise. In combinations of measurements the partially reconstructed analysis will have a larger statistical weight.

5 Summary

The LHCb collaboration continues to drive precision on the CKM angle γ , with a current average value, determined in combination with charm measurements, of $\gamma = (63.8_{-3.7}^{+3.5})^\circ$ [5]. New LHCb measurements will be included in the next combination, and those that use the self-conjugate $D \rightarrow K_S^0 h^+ h^-$, where $h = \pi, K$, final state are presented in these proceedings. An analysis of $B^0 \rightarrow DK^{*0}$ decays determined that $\gamma = (49_{-19}^{+22})^\circ$ [7] and will reduce tensions between measurements made using B^\pm and B^0 decays in the next combination. Finally, two new LHCb measurements performed using $B^\pm \rightarrow D^* K^\pm$ decays [9, 10] for the first time provide additional sensitivity to γ , as is necessary for a more precise test of CKM unitarity.

References

- [1] J. Brod and J. Zupan, *JHEP* **01**, 051 (2014).
- [2] J. Charles et al. (CKMfitter group), *Phys. Rev.* **D91**, updated results and plots available at <http://ckmfitter.in2p3.fr/>, 073007 (2015).
- [3] M. Bona et al. (UTfit collaboration), *Rend. Lincei Sci. Fis. Nat.* **34**, 37–57 (2023).
- [4] R. Aaij et al. (LHCb collaboration), *Phys. Rev. D* **97**, 031101 (2018).
- [5] R. Aaij et al. (LHCb collaboration), *JHEP* **12**, 141 (2021).
- [6] R. Aaij et al. (LHCb collaboration), LHCb-CONF-2023-004 (2023).
- [7] R. Aaij et al. (LHCb collaboration), *Eur. Phys. J. C* **84**, 206 (2024).
- [8] R. Aaij et al. (LHCb collaboration), LHCb-PAPER-2023-040, Submitted to *JHEP* (2024).
- [9] R. Aaij et al. (LHCb collaboration), *JHEP* **02**, 118 (2024).
- [10] R. Aaij et al. (LHCb collaboration), *JHEP* **12**, 013 (2023).
- [11] A. Bondar, Unpublished BINP special analysis meeting proceedings (2002).
- [12] A. Bondar and A. Poluektov, *Eur. Phys. J. C* **47**, 347–353 (2006).
- [13] A. Bondar and A. Poluektov, *Eur. Phys. J. C* **55**, 51–56 (2008).
- [14] A. Giri, Y. Grossman, A. Soffer, and J. Zupan, *Phys. Rev. D* **68**, 054018 (2003).
- [15] J. Libby et al. (CLEO collaboration), *Phys. Rev. D* **82**, 112006 (2010).
- [16] M. Ablikim et al. (BESIII collaboration), *Phys. Rev. D* **101**, 112002 (2020).
- [17] M. Ablikim et al. (BESIII collaboration), *Phys. Rev. D* **102**, 052008 (2020).
- [18] R. Aaij et al. (LHCb collaboration), *Phys. Rev.* **D93**, 112018 (2016).
- [19] R. Aaij et al. (LHCb collaboration), *JHEP* **02**, 0169 (2021).
- [20] R. Aaij et al. (LHCb collaboration), *JHEP* **06**, 131 (2016).